symmetry

Article

Unusual Temperature Evolution of Quasiparticle Band Dispersion in Electron-Doped FeSe Films

Kosuke Nakayama [1,2,*], Koshin Shigekawa [1], Katsuaki Sugawara [1,2,3,4], Takashi Takahashi [1,3,4] and Takafumi Sato [1,3,4]

1 Department of Physics, Tohoku University, Sendai 980-8578, Japan; k.shigekawa@arpes.phys.tohoku.ac.jp (K.S.); k.sugawara@arpes.phys.tohoku.ac.jp (K.S.); t.takahashi@arpes.phys.tohoku.ac.jp (T.T.); t-sato@arpes.phys.tohoku.ac.jp (T.S.)
2 Precursory Research for Embryonic Science and Technology (PRESTO), Japan Science and Technology Agency (JST), Tokyo 102-0076, Japan
3 WPI Research Center, Advanced Institute for Materials Research, Tohoku University, Sendai 980-8577, Japan
4 Center for Spintronics Research Network, Tohoku University, Sendai 980-8577, Japan
* Correspondence: k.nakayama@arpes.phys.tohoku.ac.jp

Abstract: The discovery of high-temperature (high-T_c) superconductivity in one-monolayer FeSe on $SrTiO_3$ has attracted tremendous attention. Subsequent studies suggested the importance of cooperation between intra-FeSe-layer and interfacial interactions to enhance T_c. However, the nature of intra-FeSe-layer interactions, which would play a primary role in determining the pairing symmetry, remains unclear. Here we have performed high-resolution angle-resolved photoemission spectroscopy of one-monolayer and alkaline-metal-deposited multilayer FeSe films on $SrTiO_3$, and determined the evolution of quasiparticle band dispersion across T_c. We found that the band dispersion in the superconducting state deviates from the Bogoliubov-quasiparticle dispersion expected from the normal-state band dispersion with a constant gap size. This suggests highly anisotropic pairing originating from small momentum transfer and/or mass renormalization due to electron–boson coupling. This band anomaly is interpreted in terms of the electronic interactions within the FeSe layers that may be related to the high-T_c superconductivity in electron-doped FeSe.

Keywords: iron-based superconductors; thin films; ARPES; electronic structure

check for updates

Citation: Nakayama, K.; Shigekawa, K.; Sugawara, K.; Takahashi, T.; Sato, T. Unusual Temperature Evolution of Quasiparticle Band Dispersion in Electron-Doped FeSe Films. *Symmetry* **2021**, *13*, 155. https://doi.org/10.3390/sym13020155

Received: 28 December 2020
Accepted: 18 January 2021
Published: 20 January 2021

1. Introduction

Iron selenide (FeSe) is structurally the simplest iron-based superconductor with the superconducting-transition temperature (T_c) of ~9 K [1]. Intriguingly, one-monolayer (1 ML) film of FeSe grown on $SrTiO_3$ substrate exhibits exceptionally high T_c [2]. The T_c value reported by transport measurements reaches 40 K [2,3], which is about five times higher than the bulk counterpart. In addition, Cooper pairing at a higher temperature of 65 K, which exceeds the highest T_c (56 K) ever achieved in iron-based superconductors, has been suggested from a gap-closing temperature by angle-resolved photoemission spectroscopy (ARPES) [4–7] and Meissner effect by mutual conductance measurements [8]. These observations triggered fierce debates on the origin of the T_c enhancement in 1 ML-FeSe film. One key ingredient is a novel cross-interface electron–phonon coupling. The strong coupling between electrons in the FeSe layer and optical phonons of $SrTiO_3$ has been verified via the observation of replica bands by ARPES and theoretically proposed to enhance T_c in most of possible pairing symmetries [9,10]. Later, the close link between strong electron–phonon coupling and T_c enhancement has been supported experimentally, e.g., by isotope effects [11,12]. With these findings as a guiding principle, the search for high T_c in atomically thin films of other iron-based superconductors interfaced with $SrTiO_3$ [13–15] has been accelerated. Another key ingredient for T_c enhancement is a charge transfer from $SrTiO_3$. Heavy electron doping to the FeSe layer leads to unique electronic structure consisting only of electron-like Fermi surfaces [4,5,16], in contrast to the semimetallic nature of bulk FeSe [17,18]. The electron doping is essential for the high-T_c superconductivity, as established by the observation of high T_c above 40 K even in multilayer and bulk FeSe by doping electron carriers [19–21]. Therefore, there is accumulated evidence that the FeSe layer has the capability of inducing 40-K superconductivity through electron doping and the interfacial electron–phonon coupling will assist further T_c or pairing enhancement. However, little is known about why electron doping leads to the high T_c's above 40 K. In particular, interactions within the FeSe layer, which would primarily determine the pairing symmetry, remain unclear.

In this study, we performed a comparative ARPES experiment on the surface of 1 ML- and Cs-deposited 20 ML-FeSe films on $SrTiO_3$, where the interfacial effects were present and absent, respectively. We demonstrated anomaly in the quasiparticle-band dispersions in the superconducting state, which is not expected from the Bogoliubov-quasiparticle (BQP) dispersion induced by a simple *s*-wave-gap opening. We discuss implications of our observation in relation to intra-FeSe-layer interactions.

2. Materials and Methods

The molecular beam epitaxy method was used to obtain 1 ML- and 20 ML-FeSe films; the films were grown on a TiO_2-terminated Nb(0.05 wt%)-$SrTiO_3$ substrate (SHINKOSHA) by simultaneously evaporating Fe and Se atoms while keeping a substrate temperature at 430 °C with a deposition rate of 0.01 ML/s [19]. Electron doping to 20 ML-FeSe was realized by evaporating Cs atoms onto the film surface at room temperature using a Cs dispenser (SAES Getters) [22]. After the growth, the film was transferred to the ARPES-measurement chamber without exposure to air. ARPES measurements were performed with a SES2002 spectrometer (Scienta Omicron) with the He-Iα resonance line ($h\nu$ = 21.218 eV) at Tohoku University. The film was kept under an ultrahigh vacuum of 5×10^{-11} Torr during the ARPES measurement, and no remarkable surface degradation was observed for a typical measurement time of 1 day. The energy and angular resolutions were set to be 7–12 meV and 0.2°, respectively. A gold film which made electrical contact with the film was referenced to calibrate the Fermi level (E_F).

3. Results

First, we present the electronic structure of Cs-deposited 20 ML-FeSe film measured at T = 50 K. As shown in Figure 1a,b, there was a circular-shaped large Fermi surface at the Brillouin-zone corner (M point) which originated from E_F crossing of an electron band with the bottom of the dispersion around 50 meV below E_F. The top of a hole-like band around the zone center (Γ point) was about 50 meV below E_F, resulting in the absence of a hole-like Fermi surface in contrast to the as-grown multilayer FeSe film [4,5] or bulk FeSe [17,18]. These observations confirmed a successful electron doping by Cs deposition onto the FeSe surface. The electron carrier concentration (n_e) calculated from the Fermi-surface volume was ~0.11 electrons/Fe, which corresponds to the optimal doping level with T_c value of ~40 K [22]. To investigate how the band structure changes by the superconducting transition, we performed high-resolution measurements across T_c (50 and 13 K) along a momentum (k) cut A indicated by a blue line in Figure 1a. The results displayed in Figure 1c,d show that while the electron band above T_c crossed E_F at the Fermi wave vector (k_F) of ~0.17 π/a, the band dispersion below T_c had a local maximum below E_F so as not to cross E_F due to a superconducting-gap opening. It is noted that the k location of the electron-band top below T_c coincided with the k_F point above T_c, consistent with the Cooper-pairing origin of the observed gap. The superconducting-gap opening is also clearly seen in energy distribution curves (EDCs) in Figure 1e, in which the peak position at k_F (k_3 defined in Figure 1c,d) was shifted from E_F to a high binding energy by ~10 meV with decreasing the temperature to form a superconducting gap. Since the nodeless *s*-wave superconductivity is realized in electron-doped multilayer FeSe [19,20], one can see the superconducting-gap opening below T_c irrespective of the k cut, e.g., along the k cut crossing the M point (cut B), as shown in Figure 1f–h, where essentially the same behavior with cut A was recognized.

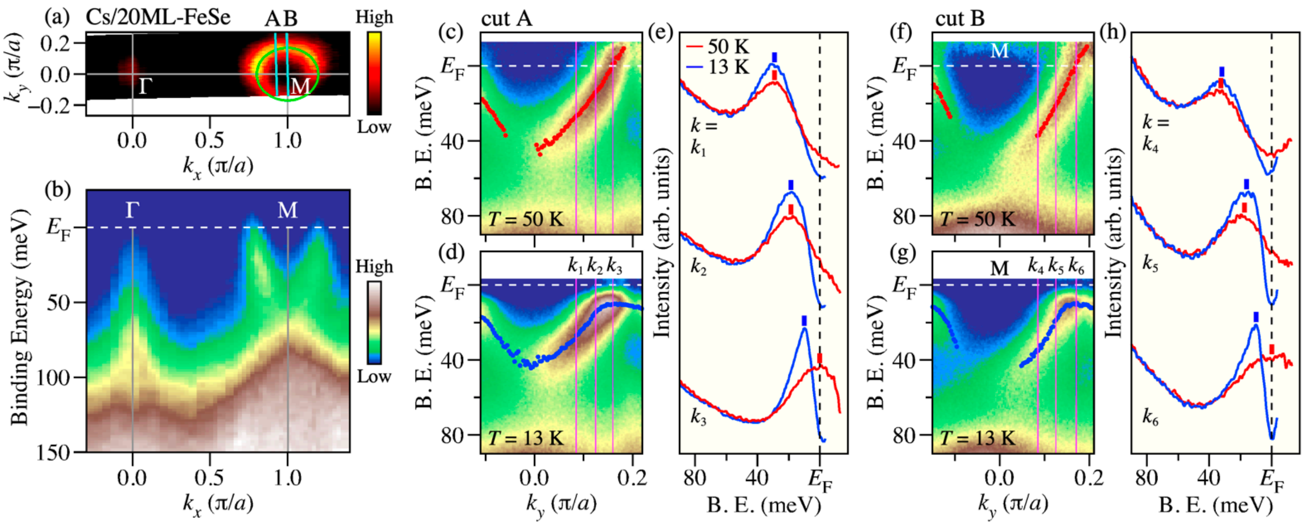

Figure 1. (**a**) ARPES intensity map at E_F as a function of two-dimensional wave vector for Cs-deposited 20 monolayer (ML)-FeSe film obtained at T = 50 K with $h\nu$ = 21.218 eV. Intensity at E_F was obtained by integrating the spectral intensity within ±10 meV of E_F. Green circle is a guide for the eyes to trace the Fermi surface. (**b**) Plot of ARPES intensity along the ΓM cut at 50 K as a function of binding energy and wave vector. (**c**,**d**) Near-E_F ARPES intensity along cut A in (**a**) at T = 50 and 13 K, respectively, divided by the Fermi–Dirac distribution (FD) function at each temperature convoluted with the resolution function. Intensity above E_F is displayed up to $3k_BT$. Red and blue circles in (**c**,**d**), respectively, are the band dispersion determined by fitting the energy distribution curves (EDCs) with Bardeen–Cooper–Schrieffer (BCS) spectral function [23]. (**e**) Comparison of EDCs between T = 50 K (red) and 13 K (blue) taken at representative k_y points [k_1, k_2, and k_3 indicated by magenta lines in (**c**,**d**)]. Red and blue dots indicate the local maxima corresponding to the peak position. (**f**–**h**) Same as (**c**–**f**) but obtained along cut B in (**a**).

An important finding manifests itself when we compare the band dispersions of the normal and superconducting states. Figure 2a displays a direct comparison of the experimental band dispersions extracted from the peak position of EDCs in cut A. As mentioned above, the band dispersion below T_c exhibited an opening of the superconducting gap and resultant bending-back behavior with the top of the dispersion at k_F. Such a characteristic band dispersion below T_c was qualitatively consistent with the dispersion relation of BQPs in the Bardeen–Cooper–Schrieffer (BCS) theory, where BQP dispersion (E_k) is expressed as $E_k = \sqrt{{\varepsilon_k}^2 + |\Delta|^2}$ (ε_k and Δ are the normal-state band dispersion and the superconducting-gap size, respectively) [24]. For a quantitative comparison, we determined ε_k by performing a polynomial fitting to the ARPES data above T_c (magenta curve) and simulated E_k by assuming a k-independent superconducting-gap size of 10 meV (light blue curve). Intriguingly, the band dispersion below T_c shows a clear deviation from the simulated BQP dispersion E_k; specifically, although the simulation predicted a finite downward energy shift of BQP dispersion compared with ε_k even in the k region far away from k_F (at least down to k_y = 0.05 π/a) because of a large Δ value with respect to the shallow electron-band bottom, the experimental dispersion below T_c became nearly identical to ε_k as soon as it moved away from k_F. Almost temperature-insensitive band position away from k_F was also clearly visible in the comparison of raw EDCs in Figure 1e (see EDCs at k_1 and k_2). The same behavior was observed at different momentum, e.g., we found that the band dispersion measured below T_c along cut B deviated from the simulated BQP dispersion over a wide k region (see Figure 2b; also see a comparison of EDCs in Figure 1h).

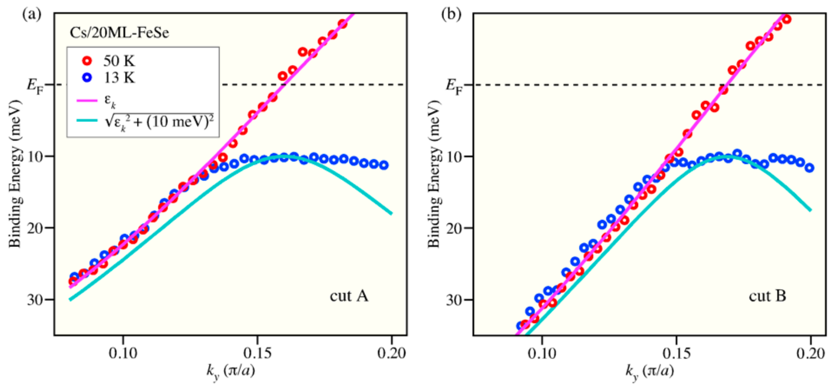

Figure 2. (**a**) Comparison of the near-E_F band dispersions in Cs-deposited 20 ML-FeSe at T = 50 K (red circles) and 13 K (blue circles) along cut A in Figure 1a. Magenta curve is the normal-state band dispersion ε_k extracted from a polynomial fitting to the red circles. Light blue curve is the calculated Bogoliubov-quasiparticle (BQP) dispersion based on the BCS formula $E_k = \sqrt{\varepsilon_k{}^2 + |\Delta|^2}$ with a constant Δ of 10 meV. (**b**) Same as (**a**) but for cut B in Figure 1a.

To clarify whether the energy difference between the experimental and simulated BQP dispersions below T_c was an essential ingredient of electron-doped high-T_c FeSe films, we investigated the band-structure evolution in 1 ML-FeSe (Figure 3). For this purpose, we performed high-resolution measurements on slightly underdoped 1 ML-FeSe (n_e = 0.09) with T_c~40 K because a sharp spectral line shape compared with the heavily doped sample (T_c~65 K; n_e~0.12) [4] is suited for accurately determining the quasiparticle band dispersion. As is well known, 1 ML-FeSe has a large electron-like Fermi surface centered at the M point. The electron band which forms the Fermi surface showed an opening of the superconducting gap (Δ~10 meV) below T_c, as highlighted by the characteristic bending-back behavior with the minimum-gap locus at k_F (see Figure 3b). A direct comparison of the band dispersions above and below T_c in Figure 3c demonstrates that an energy shift due to the superconducting-gap opening was limited to the k region around k_F~0.16 π/a (compare red and blue circles), in sharp contrast to a clear downward shift of the simulated BQP dispersion for $k_y \leq 0.1\ \pi/a$ (light blue curve). Similarly, the case of Cs-deposited 20 ML-FeSe suggested that the deviation of the experimental band dispersion from the simulated BQP dispersion below T_c is a common feature of electron-doped FeSe films irrespective of film thickness.

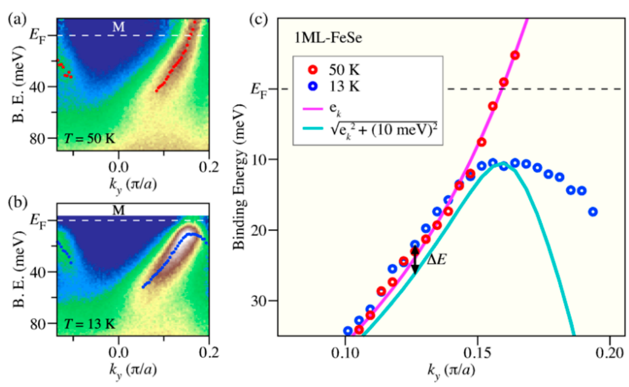

Figure 3. (**a**,**b**) ARPES intensity divided by the FD function measured along the k cut crossing the M point in 1 ML-FeSe at T = 50 K and 13 K, respectively. Red and blue circles show the band dispersion extracted from the peak position of the EDCs. (**c**) Comparison of the near-E_F band dispersions at T = 50 K (red circles) and 13 K (blue circles), together with ε_k determined by polynomial fitting to the red circles (magenta curve) and the BQP dispersion $E_k = \sqrt{\varepsilon_k{}^2 + |\Delta|^2}$ simulated with a constant Δ of 10 meV (light blue curve).

4. Discussion and Conclusions

Now we are going to discuss the origin of the observed anomaly in quasiparticle dispersion. To simulate BQP dispersion $E_k = \sqrt{\varepsilon_k{}^2 + |\Delta|^2}$, we assumed that ε_k is the same as the dispersion above T_c and Δ is k-independent. It would be natural to consider that one or both of these assumptions are incorrect, rather than thinking that the BQP picture was broken in the electron-doped FeSe. For simplicity, we consider in the following the two extreme cases that the deviation was induced by a change in either ε_k or Δ. First, to examine the k dependence of Δ as the origin, we put the experimental band dispersions below and above T_c into E_k and ε_k, respectively, and estimated $\Delta(k)$ which reproduces the experimental band dispersion below T_c. The obtained $\Delta(k)$ was strongly k-dependent as seen from Figure 4a,b for 1 ML- and Cs-deposited 20 ML-FeSe, respectively; namely, $\Delta(k)$ was finite only in the narrow k region centered at k_F (within $\pm 0.02\ \pi/a$ of k_F), so that band dispersion only around E_F was shifted toward high binding energies by the superconducting transition, consistent with our observations. An unusual Cooper pairing in the limited k space near k_F may be caused by pairing interactions which have small momentum transfer q [25–27]. For instance, it has been proposed by Migdal–Eliashberg theory for 1 ML-FeSe that forward scattering with small q phonons produces highly anisotropic superconducting gap peaked at k_F and also leads to temperature-independent band structure away from k_F [25], in qualitative agreement with $\Delta(k)$ in Figure 4a as well as band dispersion in Figure 3. Although this theory assumes a cross-interface coupling between small q phonons of $SrTiO_3$ and electrons in 1 ML-FeSe as the key pairing interactions, our observation of anisotropic $\Delta(k)$ in 20 ML-FeSe (Figure 4b) where interfacial effects are negligible suggests that small-q interactions within the FeSe layers may be also responsible for superconductivity if the k-dependent pairing was indeed a source of the deviation from the simulated BQP dispersion.

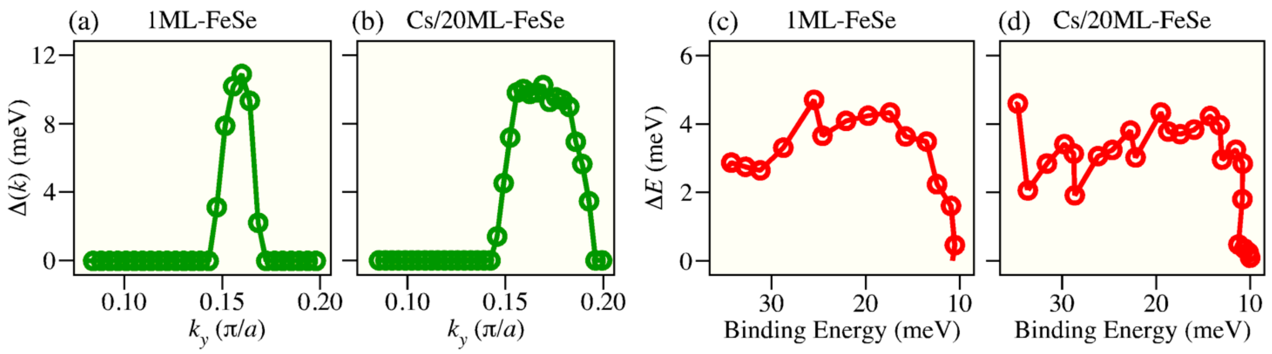

Figure 4. (**a**) k dependence of the superconducting-gap size $\Delta(k)$ which was calculated to reproduce the experimental band dispersion at 13 K for 1 ML-FeSe (blue circles in Figure 3c) with the formula $E_k = \sqrt{\varepsilon_k{}^2 + |\Delta|^2}$, where ε_k is the normal-state band dispersion extracted at T = 50 K (red circles in Figure 3c). (**b**) Same as (**a**) but for Cs-deposited 20 ML-FeSe. (**c**) Energy difference between the experimental band dispersion at 13 K (blue circles in Figure 3c) and the simulated BQP dispersion with a constant gap size of 10 meV (light blue curve in Figure 3c) in 1 ML-FeSe. (**d**) Same as (**c**) but for Cs-deposited 20 ML-FeSe.

Next, we consider another possibility that ε_k is temperature-dependent whereas k dependence of $\Delta(k)$ is small. To explain the observed deviation between the experimental and simulated BQP dispersions, ε_k below T_c must be shifted toward E_F compared with the normal-state band dispersion above T_c while keeping the same k_F position. Such an energy shift would be a consequence of mass renormalization linked to the superconducting transition, likely due to coupling with bosonic modes as reported for bulk crystals of high-T_c superconductors [28–33]. Here we defined the energy difference between the experimental and simulated BQP dispersions as ΔE (see black arrow in Figure 3c) and plotted it in Figure 4c,d for 1 ML- and 20 ML-FeSe films, respectively. As seen from Figure 4c,d, ΔE showed a broad peak around 20 meV in 1 ML- and 20 ML-FeSe. The obtained ΔE value can be used as a measure of the mass enhancement similarly to the real part of self-energies. By analogy with the fact that the peak position in the real part of self-energies below T_c corresponded to $\Delta + \Omega$, where Ω is the energy of bosonic modes coupled to electrons, the observed peak structure at ~20 meV suggests a coupling to low-energy modes with Ω~10 meV (here, Δ~10 meV). The origin of the corresponding modes is an important open question; candidates include phonons [34] and magnetic resonance [35]. Nevertheless, one important outcome from our observation is that low-energy modes intrinsic to the FeSe layer must be involved because the mass renormalization was found not only in 1 ML-FeSe, but also in 20 ML-FeSe.

In summary, we reported the evolution of low-energy band dispersion across T_c in 1 ML- and Cs-deposited 20 ML-FeSe films on $SrTiO_3$. We found deviation of the band dispersion below T_c from the simple BQP dispersion simulated with the temperature-independent ε_k and k-independent Δ. We proposed two possible scenarios as the origin of this observation; (i) anisotropic $\Delta(k)$ peaked around k_F due to the superconducting pairing by small q transfer and (ii) enhancement in the effective mass in the superconducting state due to the coupling to low-energy bosonic modes. In either scenario, the observed similarity between 1 ML- and 20 ML-FeSe suggested intra-FeSe-layer nature of the interactions. Our result lays a foundation for understanding the mechanism of high-T_c superconductivity in electron-doped FeSe.

Author Contributions: Conceptualization, K.N.; formal analysis, K.S. (Koshin Shigekawa); investigation, K.N., K.S. (Koshin Shigekawa) and K.S. (Katsuaki Sugawara); data curation, K.N. and K.S. (Koshin Shigekawa); writing—original draft preparation, K.N.; writing—review and editing, T.T. and T.S.; visualization, K.N. and K.S. (Koshin Shigekawa); project administration, K.N. and T.S.; funding acquisition, K.N., K.S. (Katsuaki Sugawara), T.T. and T.S. All authors have read and agreed to the published version of the manuscript.

Funding: This work was supported by JST-CREST (No. JPMJCR18T1) and Grant-in-Aid for Scientific Research (JSPS KAKENHI Grant Numbers JP17H04847, JP17H01139, JP18H01160, and JP20H01847).

Institutional Review Board Statement: Not applicable.

Informed Consent Statement: Not applicable.

Data Availability Statement: The data that support the findings of this study are available from the corresponding author upon request.

Acknowledgments: We thank G. Phan and M. Kuno for their assistance in the ARPES measurements.

Conflicts of Interest: The authors declare no conflict of interests.

References

1. Hsu, F.C.; Luo, J.-Y.; Yeh, K.-W.; Chen, T.-K.; Huang, T.-W.; Wu, P.M.; Lee, Y.-C.; Huang, Y.-L.; Chu, Y.-Y.; Yan, D.-C.; et al. Superconductivity in the PbO-type structure α-FeSe. *Proc. Natl. Acad. Sci. USA* **2009**, *105*, 14262–14264. [CrossRef] [PubMed]
2. Wang, Q.Y.; Wang, Q.-Y.; Li, Z.; Zhang, W.-H.; Zhang, Z.-C.; Zhang, J.-S.; Li, W.; Ding, H.; Ou, Y.-B.; Deng, P.; et al. Interface-induced high-temperature superconductivity in single unit-cell FeSe films on $SrTiO_3$. *Chin. Phys. Lett.* **2012**, *29*, 037402. [CrossRef]
3. Sun, Y.; Zhang, W.; Xing, Y.; Li, F.; Zhao, Y.; Xia, Z.; Wang, L.; Ma, X.; Xue, Q.-K.; Wang, J. High temperature superconducting FeSe films on $SrTiO_3$ substrates. *Sci. Rep.* **2014**, *4*, 6040. [CrossRef] [PubMed]
4. He, S.L.; He, S.; Zhang, W.; Zhao, L.; Liu, D.; Liu, X.; Mou, D.; Ou, Y.-B.; Wang, Q.-Y.; Li, Z.; et al. Phase diagram and electronic indication of high-temperature superconductivity at 65 K in single-layer FeSe films. *Nat. Mater.* **2013**, *12*, 605–610. [CrossRef]
5. Tan, S.Y.; Zhang, Y.; Xia, M.; Ye, Z.; Chen, F.; Xie, X.; Peng, R.; Xu, D.; Fan, Q.; Xu, H.; et al. Interface-induced superconductivity and strain-dependent spin density wave in FeSe/$SrTiO_3$ thin films. *Nat. Mater.* **2013**, *12*, 634–640. [CrossRef]
6. Peng, R.; Xu, H.C.; Tan, S.Y.; Cao, H.Y.; Xia, M.; Shen, X.P.; Huang, Z.C.; Wen, C.H.P.; Song, Q.; Zhang, T.; et al. Tuning the band structure and superconductivity in single-layer FeSe by interface engineering. *Nat. Commun.* **2014**, *5*, 5044. [CrossRef]
7. Peng, R.; Shen, X.P.; Xie, X.; Xu, H.C.; Tan, S.Y.; Xia, M.; Zhang, T.; Cao, H.Y.; Gong, X.G.; Hu, J.P.; et al. Measurement of an Enhanced Superconducting Phase and a Pronounced Anisotropy of the Energy Gap of a Strained FeSe Single Layer in FeSe/Nb:$SrTiO_3$/$KTaO_3$ Heterostructures Using Photoemission Spectroscopy. *Phys. Rev. Lett.* **2014**, *112*, 107001. [CrossRef]

8. Zhang, Z.; Wang, Y.-H.; Song, Q.; Liu, C.; Peng, R.; Moler, K.A.; Feng, D.; Wang, Y. Onset of the Meissner effect at 65 K in FeSe thin film grown on Nb-doped $SrTiO_3$ substrate. *Sci. Bull.* **2015**, *60*, 1301–1304. [CrossRef]
9. Lee, J.J.; Schmitt, F.T.; Moore, R.G.; Johnston, S.; Cui, Y.-T.; Li, W.; Yi, M.; Liu, Z.K.; Hashimoto, M.; Zhang, Y.; et al. Interfacial mode coupling as the origin of the enhancement of T_c in FeSe films on $SrTiO_3$. *Nature* **2014**, *515*, 245. [CrossRef]
10. Xiang, Y.Y.; Wang, F.; Wang, D.; Wang, Q.H.; Lee, D.H. High-temperature superconductivity at the FeSe/$SrTiO_3$ interface. *Phys. Rev. B* **2012**, *86*, 134508. [CrossRef]
11. Song, Q.; Yu, T.L.; Lou, X.; Xie, B.P.; Xu, H.C.; Wen, C.H.P.; Yao, Q.; Zhang, S.Y.; Zhu, X.T.; Guo, J.D.; et al. Evidence of cooperative effect on the enhanced superconducting transition temperature at the FeSe/$SrTiO_3$ interface. *Nat. Commun.* **2019**, *10*, 758. [CrossRef] [PubMed]
12. Rebec, S.N.; Jia, T.; Zhang, C.; Hashimoto, M.; Lu, D.-H.; Moore, R.G.; Shen, Z.-X. Coexistence of Replica Bands and Superconductivity in FeSe Monolayer Films. *Phys. Rev. Lett.* **2017**, *118*, 067002. [CrossRef] [PubMed]
13. Li, F.; Ding, H.; Tang, C.; Peng, J.; Zhang, Q.; Zhang, W.; Zhou, G.; Zhang, D.; Song, C.-L.; He, K.; et al. Interface-enhanced high-temperature superconductivity in single-unit-cell $FeTe_{1-x}Se_x$ films on $SrTiO_3$. *Phys. Rev. B* **2015**, *91*, 220503. [CrossRef]
14. Shi, X.; Han, Z.-Q.; Richard, P.; Wu, X.-X.; Peng, X.-L.; Qian, T.; Wang, S.-C.; Hu, J.-P.; Sun, Y.-J.; Ding, H. $FeTe_{1-x}Se_x$ monolayer films: Towards the realization of high-temperature connate topological superconductivity. *Sci. Bull.* **2017**, *62*, 503–507. [CrossRef]
15. Shigekawa, K.; Nakayama, K.; Kuno, M.; Phan, G.N.; Owada, K.; Sugawara, K.; Takahashi, T.; Sato, T. Dichotomy of superconductivity between monolayer FeS and FeSe. *Proc. Natl. Acad. Sci. USA* **2019**, *116*, 24470–24474. [CrossRef]
16. Liu, D.F.; Zhang, W.; Mou, D.; He, J.; Ou, Y.-B.; Wang, Q.-Y.; Li, Z.; Wang, L.; Zhao, L.; He, S.; et al. Electronic origin of high-temperature superconductivity in single-layer FeSe superconductor. *Nat. Commun.* **2012**, *3*, 931. [CrossRef]
17. Maletz, J.; Zabolotnyy, V.B.; Evtushinsky, D.V.; Thirupathaiah, S.; Wolter, A.U.B.; Harnagea, L.; Yaresko, A.N.; Vasiliev, A.N.; Chareev, D.A.; Böhmer, A.E.; et al. Unusual band renormalization in the simplest iron-based superconductor $FeSe_{1-x}$. *Phys. Rev. B* **2014**, *89*, 220506. [CrossRef]
18. Nakayama, K.; Miyata, Y.; Phan, G.N.; Sato, T.; Tanabe, Y.; Urata, T.; Tanigaki, K.; Takahashi, T. Reconstruction of Band Structure Induced by Electronic Nematicity in an FeSe Superconductor. *Phys. Rev. Lett.* **2014**, *113*, 237001. [CrossRef]
19. Miyata, Y.; Nakayama, K.; Sugawara, K.; Sato, T.; Takahashi, T. High-temperature superconductivity in potassium-coated multilayer FeSe thin films. *Nat. Mater.* **2015**, *14*, 775–779. [CrossRef]
20. Wen, C.H.P.; Xu, H.C.; Chen, C.; Huang, Z.C.; Lou, X.; Pu, Y.J.; Song, Q.; Xie, B.P.; Abdel-Hafiez, M.; Chareev, D.A.; et al. Anomalous correlation effects and unique phase diagram of electron-doped FeSe revealed by photoemission spectroscopy. *Nat. Commun.* **2016**, *7*, 10840. [CrossRef]
21. Shiogai, J.; Ito, Y.; Mitsuhashi, T.; Nojima, T.; Tsukazaki, A. Electric-field-induced superconductivity in electrochemically etched ultrathin FeSe films on $SrTiO_3$ and MgO. *Nat. Phys.* **2016**, *12*, 42–46. [CrossRef]
22. Phan, G.N.; Nakayama, K.; Kanayama, S.; Kuno, M.; Sugawara, K.; Sato, T.; Takahashi, T. ARPES study of cesium-coated FeSe thin films on $SrTiO_3$. *J. Phys. Conf. Ser.* **2017**, *871*, 012017. [CrossRef]
23. Norman, M.R.; Randeria, M.; Ding, H.; Campuzano, J.C. Phenomenology of the low-energy spectral function in high-T_c superconductors. *Phys. Rev. B* **1998**, *57*, R11093–R11096. [CrossRef]
24. Matsui, H.; Sato, T.; Takahashi, T.; Wang, S.-C.; Yang, H.-B.; Ding, H.; Fujii, T.; Watanabe, T.; Matsuda, A. BCS-Like Bogoliubov Quasiparticles in High-T_c Superconductors Observed by Angle-Resolved Photoemission Spectroscopy. *Phys. Rev. Lett.* **2003**, *90*, 217002. [CrossRef] [PubMed]
25. Wang, Y.; Nakatsukasa, K.; Rademaker, L.; Berlijn, T.; Johnston, S. Aspects of electron–phonon interactions with strong forward scattering in FeSe Thin Films on $SrTiO_3$ substrates. *Supercond. Sci. Technol.* **2016**, *29*, 054009. [CrossRef]
26. Yamase, H.; Zeyher, R. Superconductivity from orbital nematic fluctuations. *Phys. Rev. B* **2013**, *88*, 180502. [CrossRef]
27. Agatsuma, T.; Yamase, H. Structure of the pairing gap from orbital nematic fluctuations. *Phys. Rev. B* **2016**, *94*, 214505. [CrossRef]
28. Norman, M.R.; Ding, H.; Campuzano, J.C.; Takeuchi, T.; Randeria, M.; Yokoya, T.; Takahashi, T.; Mochiku, T.; Kadowaki, K. Unusual Dispersion and Line Shape of the Superconducting State Spectra of $Bi_2Sr_2CaCu_2O_{8+\delta}$. *Phys. Rev. Lett.* **1997**, *79*, 3506–3509. [CrossRef]
29. Valla, T.; Fedorov, A.V.; Johnson, P.D.; Wells, B.O.; Hulbert, S.L.; Li, Q.; Gu, G.D.; Koshizuka, N. Evidence for Quantum Critical Behavior in the Optimally Doped Cuprate $Bi_2Sr_2CaCu_2O_{8+\delta}$. *Science* **1999**, *285*, 2110. [CrossRef]
30. Kaminski, A.; Randeria, M.; Campuzano, J.C.; Norman, M.R.; Fretwell, H.; Mesot, J.; Sato, T.; Takahashi, T.; Kadowaki, K. Renormalization of Spectral Line Shape and Dispersion below T_c in $Bi_2Sr_2CaCu_2O_{8+\delta}$. *Phys. Rev. Lett.* **2001**, *86*, 1070. [CrossRef]
31. Lanzara, A.; Bogdanov, P.V.; Zhou, X.J.; Kellar, S.A.; Feng, D.L.; Lu, E.D.; Yoshida, T.; Eisaki, H.; Fujimori, A.; Kishio, K.; et al. Evidence for ubiquitous strong electron–phonon coupling in high-temperature superconductors. *Nature* **2001**, *412*, 510. [CrossRef] [PubMed]
32. Richard, P.; Sato, T.; Nakayama, K.; Souma, S.; Takahashi, T.; Xu, Y.-M.; Chen, G.F.; Luo, J.L.; Wang, N.L.; Ding, H. Angle-Resolved Photoemission Spectroscopy of the Fe-Based $Ba_{0.6}K_{0.4}Fe_2As_2$ High Temperature Superconductor: Evidence for an Orbital Selective Electron-Mode Coupling. *Phys. Rev. Lett.* **2009**, *102*, 047003. [CrossRef] [PubMed]
33. Koitzsch, A.; Inosov, D.S.; Evtushinsky, D.V.; Zabolotnyy, V.B.; Kordyuk, A.A.; Kondrat, A.; Hess, C.; Knupfer, M.; Büchner, B.; Sun, G.L.; et al. Temperature and Doping-Dependent Renormalization Effects of the Low Energy Electronic Structure of $Ba_{1-x}K_xFe_2As_2$ Single Crystals. *Phys. Rev. Lett.* **2009**, *102*, 167001. [CrossRef] [PubMed]

34. Tang, C.; Liu, C.; Zhou, G.; Li, F.; Ding, H.; Li, Z.; Zhang, D.; Li, Z.; Song, C.; Ji, S.; et al. Interface-enhanced electron-phonon coupling and high-temperature superconductivity in potassium-coated ultrathin FeSe films on $SrTiO_3$. *Phys. Rev. B* **2016**, *93*, 020507. [CrossRef]
35. Ma, M.; Bourges, P.; Sidis, Y.; Xu, Y.; Li, S.; Hu, B.; Li, J.; Wang, F.; Li, Y. Prominent Role of Spin-Orbit Coupling in FeSe Revealed by Inelastic Neutron Scattering. *Phys. Rev. X* **2017**, *7*, 021025. [CrossRef]